Available online at www.sciencedirect.com
ScienceDirect
Journal of Power Sources 174 (2007) 462–468
JOURNAL OF POWER SOURCES
www.elsevier.com/locate/jpowsour

Surface film formation on electrodes in a $LiCoO_2$/graphite cell: A step by step XPS study

R. Dedryvère [a], H. Martinez [a,*], S. Leroy [a], D. Lemordant [b], F. Bonhomme [c], P. Biensan [c], D. Gonbeau [a]

[a] *LCTPCM, Université de Pau, Hélioparc Pau Pyrénées, 2 av. Pierre Angot, 64053 Pau Cedex 9, France*
[b] *CIME (EA2098), Université F. Rabelais, Parc de Grandmont, 37200 Tours, France*
[c] *SAFT, 111 bd Alfred Daney, 33074 Bordeaux Cedex, France*

Available online 22 June 2007

Abstract

In this paper, we report on a study of the electrode/electrolyte interfaces of a $LiCoO_2$/C cell using XPS (X-ray photoelectron spectroscopy). The originality of our work lies in detailed investigations step by step during the first cycle. The results have shown that the formation process of the SEI takes place in different successive stages that are dependent on the potential of the cell. It clearly appears that SEI formation continues in the potential range where lithium ion intercalation proceeds in the carbon electrode. Salt degradation products are formed after solvent decomposition ones. Concerning the $LiCoO_2$/electrolyte interface, the results obtained have shown the formation of a very thin film on the active material but not on the binders. In all cases, the novel XPS approach applied in the lab, combining core peaks and valence band analyses, allows a precise characterization of the main chemical species of the interface layers. On the basis of these results and in conjunction with literature data, the degradation mechanisms have been discussed.

Keywords: Li-ion cells; Interface; XPS; SEI; $LiCoO_2$; Graphite

1. Introduction

Most commercial lithium-ion cells manufactured today consist of a graphitic carbon based negative electrode, a positive lithium metal oxide electrode and a separator soaked with an electrolyte based on a solution of lithium salt in a mixture of two or more organic solvents. The possibility of a thermodynamically stable electrolyte is actually non-existent and it is the chemical passivation of the surfaces that ensures the inertness of the bulk electrolyte.

Over the past decades, numerous research efforts have been focused on the so called solid electrolyte interphase (SEI) which develops at the negative electrode of Li-ion cells, as the result of electrolyte degradation processes [1–3]. The nonreversibility and self-limiting nature of this passivation process have greatly contributed to the development of the Li-ion technology. Compared with the SEI research interest, there have been relatively few studies dedicated to the understanding of the positive electrode/electrolyte interface.

The characterization of the key attributes of the corresponding surface chemistries appears rather difficult due to the low thickness together with air sensitivity of electrode/electrolyte interfaces, and it is becoming obvious that addressing the interfacial issues necessitates suitable tools. During last years, many authors have studied the interface phenomena by means of various surface analysis techniques (FTIR, XPS, Raman, AFM, ...) and many research trends have been aimed at controlling the influence of different parameters (electrolyte, additives, temperature, aging, cycling, ...). However, the formation mechanisms of the interfaces as well as their composition and nature are still subject to numerous controversial discussions.

In addition, it is to be noted that many works have been conducted on non-active electrodes clearly different (surface areas, functionalities) from the composite electrode materials used in batteries.

In this paper, we investigate the processes of formation of the SEI step by step during the electrochemical insertion and de-

* Corresponding author.
E-mail address: herve.martinez@univ-pau.fr (H. Martinez).

0378-7753/$ – see front matter © 2007 Elsevier B.V. All rights reserved.
doi:10.1016/j.jpowsour.2007.06.033

insertion of lithium ions into graphite and $LiCoO_2$ electrodes using X-ray photoelectron spectroscopy (XPS).

2. Experimental

The graphite electrodes, a mixture of synthetic graphite flakes ($d_{50} = 22\,\mu m$) and mesocarbon microbeads (MCMB, $d_{50} = 10.2\,\mu m$), were kindly provided by SAFT as well as cobalt electrodes ($LiCoO_2$). The active material of the negative electrode is deposited on a Cu foil. For mechanical stability, the graphite powder is mixed with two binders: styrene butadiene rubber (SBR) and carboxymethyl cellulose (CMC). The positive electrode consists of $LiCoO_2$ mixed with PVDF and carbon black, deposited on a Al foil. The electrolyte EC/DEC/DMC (2/1/2) (ethylene, diethyl and dimethyl carbonates) + $LiPF_6$ (1 M) was purchased from Merck (Selectipur®) and the water content of the solvents was less than 20 ppm as indicated by the manufacturer. Graphite/Li_xCoO_2 cells were built using Swagelok connectors and cycled with an Arbin battery cycler. Charge and discharge were operated in the galvanostatic mode at C/20 rate with a current density of 177 $\mu A\,cm^{-2}$ (a C/20 rate corresponds to a current density at which the full capacity of the cell can be charged – or discharged – in 20 h). Charge was operated to a cut-off voltage of +4.3 V and discharge to a cut-off voltage of +2.5 V. For surface studies during cycling, both electrodes were carefully separated from the rest of the battery components, washed with DMC to remove the electrolyte, and dried prior to being packed into a hermetical sealed glass tube for transportation. All the operation was done in a glove box under Argon atmosphere.

To prevent the samples from moisture/air exposure on the analysis site, the XPS spectrometer was directly connected through a transfer chamber to a nitrogen dry-box so that the electrodes could be easily removed from the tube within the dry-box, and placed on the sample holder without any contamination.

XPS analyses were carried out with a Kratos Axis Ultra spectrometer using a focused monochromatized Al Kα radiation ($h\nu = 1486.6$ eV). The spectrometer was calibrated using the photoemission line Ag $3d_{5/2}$ (binding energy 368.3 eV). For the Ag $3d_{5/2}$ line the full width at half maximum (FWHM) was 0.58 eV under the recording conditions. Core peaks and valence band spectra were recorded with 20 eV constant pass energy. The analyzed area of the samples was 300 $\mu m \times 700\,\mu m$, and the pressure in the analysis chamber was ca. 5×10^{-7} Pa. No charge neutralization was used. Short-time spectra were recorded at the beginning and at the end of each experiment to check the non-degradation of the samples in the X-ray beam. Peaks assignments were made with respect to reference compounds, namely $LiPF_6$, LiF, Li_2CO_3, polyethylene oxide PEO $(–CH_2–CH_2–O–)_n$, CH_3OCO_2Li and $OP(OCH_3)_3$. The binding energy scale was calibrated from the carbon contamination using the C 1s peak at 285.0 eV. Core peaks were analyzed using a non-linear Shirley-type background [4], and peak positions and areas were obtained by a weighed least-square fitting of model curves (70% Gaussian, 30% Lorentzian) to the experimental data. Quantification is performed on the basis of Scofield's relative sensitivity factors [5].

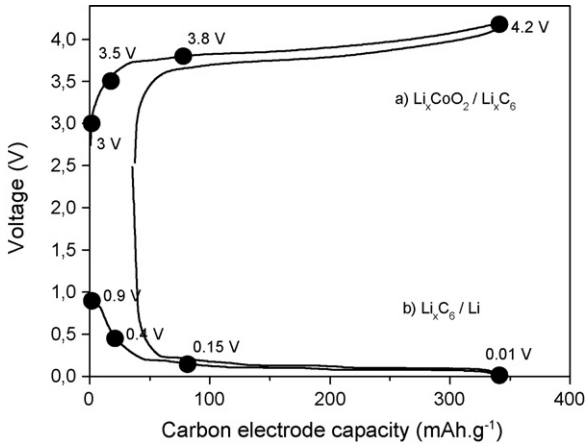

Fig. 1. (a) First cycle of charge/discharge of the operating cell ($LiCoO_2/Li_xC_6$) studied in this work, (b) corresponding potential of the negative electrode vs. Li^+/Li.

3. Results

Fig. 1 shows the first cycle of charge/discharge of the operating cell ($LiCoO_2/Li_xC_6$) studied in this work. In order to analyze precisely the mechanism of the SEI layer formation at the electrode's surface, the electrochemical reaction was stopped after the first charge of the cell at 3.0, 3.5, 3.8 and 4.2 V, corresponding for the negative graphite electrode to 0.9, 0.4, 0.15 and 0.01 V versus Li^+/Li, respectively (Fig. 1b). Each composite electrode was recovered from the cell after electrochemical reaction and washed by DMC.

3.1. Negative electrode

Fig. 2 shows the C 1s and F 1s core peaks of composite graphite electrodes recovered from the cells after a first charge

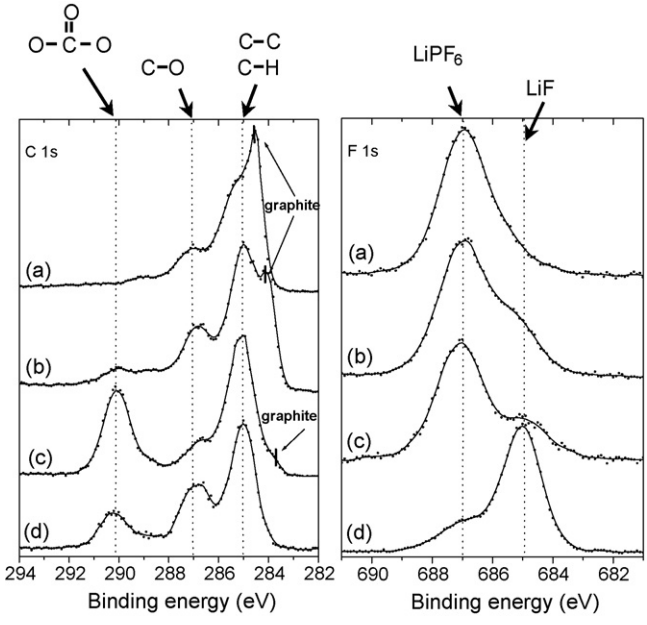

Fig. 2. C 1s and F 1s XPS spectra of the composite negative electrode stopped at: (a) 3 V, (b) 3.5 V, (c) 3.8 V and (d) 4.2 V during the first charge.

Table 1
Binding energy (eV) and atomic percentages from XPS spectra of the negative electrode during the first charge

	3.0 V		3.5 V		3.8 V		4.2 V	
	BE (eV)	%	BE (eV)	%	BE (eV)	%	BE (eV)	%
C 1s	284.5	23	284.2	8	283.7	0.9	–	–
	285.1	27	285.0	26	285.0	16	285.0	11
	287.0	16	286.9	11	286.7	5	286.9	7
	289.0	2.9	288.8	2.7	288.7	1	288.8	1
	–	–	290.1	3.5	290.0	11	290.2	3.4
O 1s	532.2	7	532.4	12	532.6	28	531.6	20
	533.6	8	533.8	10	533.5	9	533.5	7
F 1s	684.9	1	685.1	3	684.9	1	685.0	17
	686.9	7	686.9	9	687.1	3	686.9	4
P 2p	134.5	0.4	134.1	0.6	134.2	0.2	134.3	2.6
	137.2	1.7	137.2	2.2	137.3	0.9	137.1	1
Li 1s	56.4	6	56.1	12	55.8	24	56.0	26

at: (a) 3.0 V, (b) 3.5 V, (c) 3.8 V and (d) 4.2 V. Results of quantitative analysis of these samples are reported in Table 1. For a non-exhaustive presentation, P 2p and Li 1s are not presented. Furthermore, O 1s core peaks are not shown here as they provide very poor information, since all oxygen-containing species present at the surface layer contribute to the observed spectrum, with very few variations in binding energy.

The C 1s spectrum of sample (a) (Fig. 2) displays a narrow main peak observed at 284.5 eV which is assigned to graphite. At 3.5 V, the intensity of the graphite peak is smaller, suggesting that the SEI formation process has just started. Then, upon charge and insertion of lithium ions, we can observe a progressive decrease of this peak which is hardly detectable after charge at 3.8 V and completely disappears at 4.2 V. Taking into account the XPS depth analysis (≈5 nm), we estimate that the SEI formed at the end of the first charge is thicker than 5 nm.

In addition to the graphite peak, three main peaks can be observed during the charge: the first at 285.0 eV is attributed to hydrocarbon contamination and to carbon atoms bound only to C or H atoms. The second, at 286.8 eV, is attributed to carbon atoms in a one-oxygen environment, while the third, at 290.1 eV, is assigned to carbon atoms in a three-oxygen environment. This latter is due to the presence of carbonate species, which can be Li_2CO_3 and/or lithium alkyl carbonates $ROCO_2Li$. The peak at 286.8 eV can be attributed to lithium alkyl carbonates ($R–CH_2–OCO_2Li$). Such lithium alkyl carbonate species have been widely described as the main components of the SEI forming on graphite negative electrodes [6,7]. However, in $ROCO_2Li$ species the number of carbon atoms bound to three oxygens and bound to one oxygen are the same. Now, if we consider sample (b) obtained after charge at 3.5 V, the peak intensity at 286.8 eV is much higher than that at 290.1 eV. It can thus not be due only to the presence of Li alkyl carbonates species, for which both peaks would exhibit the same intensity. The peak at 286.8 eV could be explained by the presence of oligomeric species of polyethylene oxide PEO $(–CH_2–CH_2–O–)_n$, for which all carbon atoms are in a one-oxygen environment, or ROLi species. Those compounds have already been detected at the surface of various electrodes [8–10].

After charging the cell at 3.8 V (sample c), the peak at 290.1 eV appears clearly more intense than that at 286.8 eV, in opposition to previous sample. This peak is therefore mainly due to Li_2CO_3, while the small peak at 286.8 eV is explained by the presence of a small amount of Li alkyl carbonates and/or PEO oligomers.

Finally, after full charge at 4.2 V carbon-containing species at the surface are mainly Li alkyl carbonates $ROCO_2Li$ or a mixture of Li_2CO_3 and $ROCO_2Li$, probably associated to a small amount of PEO oligomers $(–CH_2–CH_2–O–)_n$ or ROLi species. Note that an additional weak component (1–3%) at 288.7–289.0 eV was necessary to fully interpret the shape of these C 1s spectra (see Table 1). This component can be assigned to carbon atoms in a two-oxygen environment, and could be explained by a small amount of oxalates at the surface. Their formation mechanism has been discussed previously [10] and could be due to solvents decomposition reactions leading to the formation of CO_2.

The F 1s core peaks (Fig. 2) of the same samples consist of two peaks (687.0 and 685.0 eV), respectively assigned to the salt $LiPF_6$, and to LiF. Upon charge, we can observe an increase in LiF peak. Results of quantitative analysis reported in Table 1 show that this increase is very important between 3.8 and 4.2 V. The evolution of these spectra agrees with the deposition at the very end of the charge of an important quantity of LiF, which becomes the main component of the outer part of the SEI.

The P 2p spectra of the same samples are made of two unresolved doublets ($2p_{3/2}$ and $2p_{1/2}$, with a spin-orbit splitting of about 0.8–0.9 eV). The first peak (137.2 eV) is attributed to $LiPF_6$ while the second one (134.3 eV) corresponds to the presence of phosphates due to the decomposition of $LiPF_6$. Further characterization of these phosphates is rather difficult by XPS. We can just affirm that the observed P atoms are in a four-oxygen environment, but they can be present in different forms such as PO_4^{3-} ions or $OP(OR)_3$ where R is an alkyl chain [10]. Upon charge, we observe an increase of the phosphate peak intensity, which mainly occurs between 3.8 and 4.2 V. These results are in agreement with the observations of F 1s spectra. Indeed, both LiF and phosphates come from the degradation of $LiPF_6$. Therefore, the $LiPF_6$ decomposition mainly occurs between 3.8 and 4.2 V.

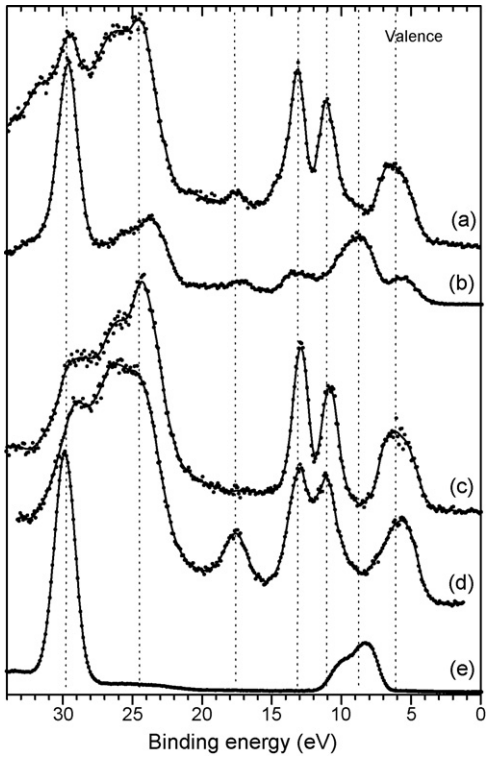

Fig. 3. XPS valence spectra of the composite negative electrode stopped at: (a) 3.8 V and (b) 4.2 V, and valence spectra of reference compounds (c) Li_2CO_3, (d) CH_3OCO_2Li, (e) LiF.

The Li 1s spectra exhibit weak variations in their binding energy (between 55.7 and 56.3 eV). However, a slight shift towards lower binding energies from 3.0 to 3.8 V and a shift towards higher binding energies at 4.2 V. Taking into account that the Li 1s peaks of Li_2CO_3, LiF and $LiPF_6$ are respectively located at 55.5, 56.0 and 56.9 eV, the position of the maximum depends on the composition of the Li-containing species mixture (see Table 1). The progressive decrease of the binding energy up to 3.8 V is in agreement with the increase of the amount of Li_2CO_3 observed before, while the final increase in binding energy at 4.2 V is in agreement with the appearance of LiF.

XPS valence band spectra, which correspond to the visualization of the occupied density of states are rarely used, especially in this kind of electrode/electrolyte interface study. Recording and interpretation of these data require careful and patient experimentation but they present very interesting potentialities. Indeed, they are scrutinizing the less bound electrons of the materials, those that are directly involved in the bonds between atoms and consequently that contain the highest potential information. Their detailed analysis would need band structure calculations and especially theoretical density of states. However, we can use valence band (VB) spectra as fingerprints to identify a species (or a few mixing of species), which constitutes a complementary approach from the core peaks analysis.

The valence spectra at 3.8 and 4.2 V are presented on Fig. 3. We added the valence spectra of LiF and of the reference carbonate species Li_2CO_3, and CH_3OCO_2Li (as an example for $ROCO_2Li$ species which have very similar spectra [11]). For the reference compounds, the following comments could be made: The spectrum of Li_2CO_3 consists of a broad peak at 5–7 eV, two narrow peaks at 11 and 13 eV, and a large massif with a narrow maximum at 24–25 eV. The spectrum of CH_3OCO_2Li is very similar to that of Li_2CO_3 with a characteristic additional peak at 17.6 eV and a decrease of the narrow maximum at 24–25 eV reduced to a shoulder. For LiF, two distinct massifs are identified: the first is a narrow band with a high intensity towards 30 eV; the second corresponds to a band of which the maximum of intensity is observed towards 8 eV. We also note a significant shoulder towards high binding energies (10 eV).

At 3.8 V, the spectrum (Fig. 3) is very close to that of Li_2CO_3. Only two differences can be noticed: (i) the peak at 29–30 eV which can be attributed to the presence of LiF, and (ii) the small peak at 17–18 eV which can be attributed to a small amount of lithium methyl carbonate CH_3OCO_2Li, as shown in a previous paper [12]. As a result, the surface of this electrode is definitely mainly made up of Li_2CO_3 and, to a lesser extent, of LiF and CH_3OCO_2Li. In the spectrum of the sample charged at 4.2 V, the valence shape of LiF with both main peaks at 29–30 eV and 8–10 eV can be recognized. Less clearly defined peaks can also be noticed: the massif at 22–27 eV and the small peaks at 17–18 eV, 13 eV and 5–6 eV*** which are consistent with the presence of CH_3OCO_2Li, or of a mixture of Li_2CO_3/CH_3OCO_2Li. As a result, the surface of this sample mainly consists of LiF and, to a lesser extent, of CH_3OCO_2Li and probably Li_2CO_3. The whole of these conclusions are consistent with the analysis of C 1s and F1s core peak spectra.

3.2. Positive electrodes

For each potential of the first charge, the positive electrodes have been studied by XPS in the same conditions as negative electrodes. Fig. 4 shows O 1s, F 1s and Li 1s core peaks at each step. Only spectra that show a significant change have been displayed. Results of quantitative analysis for all core peaks are reported in Table 2. Most of the signal (>60%) is due to the electrode additives (carbon black and PVDF), although they are in minority in the electrode (surface effect).

O 1s spectra show a progressive decrease of the narrow peak at 529.2 eV, which is related to the active material $Li_{1-x}CoO_2$ (note that most of lithium is extracted from $LiCoO_2$ between 3.8 and 4.2 V). This peak decreases from 3.3% down to 1.8%. Simultaneously, the cobalt signal decreases from 1.7% down to 1%. This result shows that the active material has been covered by a surface film during the first charge. However, this film looks thinner than for the negative electrode, since O 1s and Co 3p (and 2p) peaks characteristic of $Li_{1-x}CoO_2$ still can be observed at 4.2 V. Moreover, the O 1s/Co 3p ratio still remains close to 2, which shows that the oxygen/cobalt stoichiometry is retained upon charge. Other O 1s peaks (530–534 eV) can be assigned to numerous organic and inorganic oxygen-containing species that may be present at the surface of the electrode. It is rather difficult to clearly identify them.

F 1s spectra consist of two peaks. The first one at 687–688 eV is assigned to PVDF binder and possible traces of salt $LiPF_6$. The second one at 685 eV is assigned to LiF. The amount of LiF progressively increases from 9–10% at 3 V up to 18% at

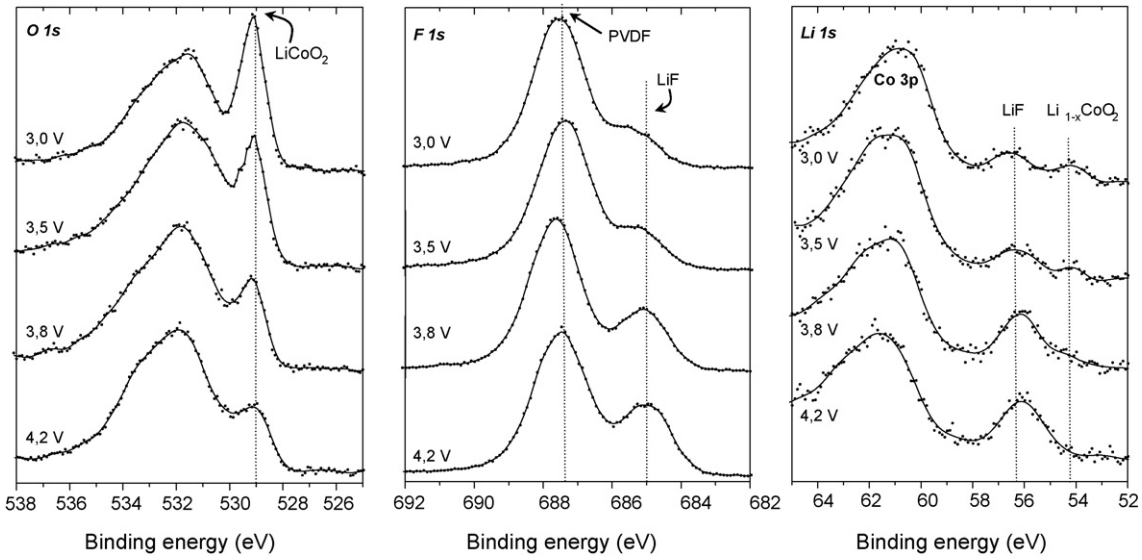

Fig. 4. O 1s, F 1s and Li 1s XPS spectra of the positive electrode stopped at: (a) 3.0 V, (b) 3.5 V, (c) 3.8 V and (d) 4.2 V during the first charge.

Table 2
Binding energies (eV) and atomic percentages from XPS spectra of the positive electrode during the first charge

	3.0 V		3.5 V		3.8 V		4.2 V	
	BE (eV)	%	BE (eV)	%	BE (eV)	%	BE (eV)	%
C 1s	284.8	23	285	21	285	20	285.2	22
	286.3	19	286.3	16	286.4	16	286.5	11
	287.7	2.3	287.6	3	288.1	2.4	287.5	2.8
	289.1	1.8	289	2.3	289.1	1.3	288.8	3.2
	290.9	9	290.9	9	290.9	10	290.9	8.4
Co 3p	60.7	1.7	60.9	1.6	60.9	1	61.1	1
O 1s	529.1	3.3	529.1	2	529.2	1.8	529.2	1.8
	532.1	4	532.2	6.8	532.2	6.3	532.4	5.4
	533.9	2.7	534.1	3	534.5	2.5	534.3	3
F 1s	685.6	4.7	685.6	5	685.2	8	685.3	8.7
	687.8	21	687.9	22	687.9	21	687.8	22
P 2p	134.7	0.3	134.8	1	134.7	1	134.7	0.9
	136.9	0.4	136.9	0.3	137	0.2	137	0.4
Li 1s	54.7	2	54.4	2	54.6	1.3	54.3	0.2
	56.6	4.8	56.4	5	56.2	7.2	56.2	9.2

4.2 V. Therefore, the amount of LiF is greater at the surface of the positive electrode than for the negative one, except at the end of charge (34% for the carbonaceous electrode).

The analysis of Li 1s core peaks confirms the evolution of the LiF amount at the surface by the increase of the 56 eV component. LiF seems to be the major constituent of the passivation film at the surface of the electrode. The second peak at 54.5 eV assigned to $Li_{1-x}CoO_2$ decreases at the end of charge (4.2 V), which can be explained by the extraction of Li^+ ions from $LiCoO_2$ (mainly between 3.8 and 4.2 V). C 1s spectra have not been displayed since they show a very poor evolution. They are mainly due to the electrode binders PVDF and carbon black. The amount of these both compounds as measured by XPS at the surface of the electrode do not change upon charge, contrary to the amount of active material that decreases. This result shows that no surface film is forming at the surface of the electrode binders, and that this passivation film preferentially forms at the surface of the active material $LiCoO_2$.

4. Discussion and conclusion

The XPS analyses carried out at the first charge show that surface films comprising electrolyte reaction products are formed on both positive and negative electrodes. These results agree with the conclusions of a previous XPS study on $LiNi_{0.8}Co_{0.2}O_2$/graphite cell [13], reporting data after three charge/discharge cycles. Our XPS results allow to make an assessment of the main species identified according to the state of charge:

Between 3 and 3.8 V, for the negative electrode, the main observed phenomenon is the formation of Li_2CO_3, associated with a small but significant quantity of CH_3OCO_2Li.

Note that we have never identified $C_2H_5OCO_2Li$ species (degradation product of DEC). This could be related to the more important solubility of the $ROCO_2Li$ species when R is an alkyl with a more important size than CH_3 [14].

Several mechanisms were reported to explain the formation of Li_2CO_3 and CH_3OCO_2Li by a reduction process (mono or bielectronic) of the electrolyte solvents:

$$EC : (CH_2O)_2CO + 2e^- + 2Li^+ \rightarrow Li_2CO_3 + C_2H_{4(g)} \quad (1)$$

$$DMC : CH_3OCO_2CH_3 + 2e^- + 2Li^+ \rightarrow Li_2CO_3 + C_2H_{6(g)} \quad (2)$$

$$DMC : 2CH_3OCO_2CH_3 + 2e^- + 2Li^+ \rightarrow 2CH_3OCO_2Li + C_2H_{6(g)} \quad (3)$$

$$DEC : C_2H_5OCO_2C_2H_5 + 2e^- + 2Li^+ \rightarrow Li_2CO_3 + C_4H_{10(g)} \quad (4)$$

The mechanism (1) could be privileged if we take into account the results from Novak et al. [15,16] on carbonaceous electrodes (electrolyte EC/DMC (1:1), $LiPF_6$ 1 M). The authors have identified, by in situ mass spectrometry, the ethylene release as being the main process at 0.8 V (versus Li^+/Li). Thus, it would seem that the preferential processes occurring on the negative electrode are a bielectronic mechanism of EC reduction (formation of Li_2CO_3) and a monoelectronic reduction of DMC (formation of CH_3OCO_2Li).

In addition, it is to be noted that these results agree with the understanding of SEI formation on graphite anodes. Indeed, the main contribution to the irreversible charge consumption is reported for graphite electrodes between 0.8 and 0.2 V versus Li^+/Li. Then, we can conclude that the main SEI formation occurs in this region. The important deposition phenomena observed at 3.5 and 3.8 V (0.4 and 0.15 V versus Li^+/Li) agree rather well with this conclusion.

For the positive electrode, between 3 and 3.8 V, a LiF deposit was observed. This deposit, present at 3 V (∼9% of LiF) increases between 3.5 and 3.8 V (∼16%) and still remains more important than for the negative electrode in this potential range. If the LiF formation can be explained by a hydrolysis of $LiPF_6$:

$$LiPF_6 + H_2O \rightarrow LiF + POF_3 + CO_2 \quad (5)$$

another possibility would be the de-intercalation of Li^+ ions of the positive electrode, due to the contact with the electrolyte, and their association with F^- ions, present in the electrolyte and migrating towards the positive electrode. These F^- ions could result from the following reaction: $PF_6^- \Leftrightarrow PF_5 + F^-$. Then, the local over-concentration in Li^+ and F^- ions would involve the precipitation of LiF on the positive electrode.

Between 3.8 and 4.2 V, for the negative electrode, the main phenomenon observed is a large deposit of LiF (34% at 4.2 V). Other mechanisms (including the salt reaction with products such as Li_2CO_3) than the hydrolysis of $LiPF_6$ could explain the formation of LiF.

$$LiPF_6 \rightarrow LiF + PF_5 \quad (6)$$

$$PF_5 + Li_2CO_3 \rightarrow 2LiF + POF_3 + CO_2 \quad (7)$$

$$LiPF_6 + Li_2CO_3 \rightarrow 3LiF + POF_3 + CO_2 \quad (8)$$

$$Li_2CO_3 + 2HF \rightarrow 2LiF + CO_2 + H_2O \quad (9)$$

However, none of these reactions (5)–(9) is directly associated with an electrochemical lithium intercalation. The important deposit of LiF during the charge between 3.8 and 4.2 V could be related to an increase of the solution acidity at the end of the charge (acidity initially present in the electrolyte: 50 ppm in HF equivalent [17]). According to the potential and the temperature, a weak oxidation of solvent would occur and protons would be released at the positive electrode. These protons would join F^- ions to form H_2F_2 species (would give HF or HF_2^-). By migration (HF_2^-) or diffusion, these acid species can reach the negative electrode where the reaction (9) would occur.

Finally, we have displayed, by a step by step XPS study, the potential-dependent character of the formation of the species making up the interfacial layers at the surface of the positive and negative electrodes. Such new approach constitutes an additional powerful tool for a better understanding of electrode–electrolyte interfaces, that could be a great help in mastering the interfacial issues.

Acknowledgment

The authors wish to thank SAFT company for electrode manufacture and financial support.

References

[1] E. Peled, D. Golodnitsky, G. Ardel, J. Electrochem. Soc. 144 (1997) L208.
[2] G. Nazri, R.H. Muller, J. Electrochem. Soc. 132 (1985) 2050.
[3] D. Aurbach, M.L. Daroux, P. Faguy, W.E. Yeager, J. Electrochem. Soc. 134 (1987) 1611–1620.
[4] D.A. Shirley, Phys. Rev. B 5 (1972) 4709.
[5] J.H. Scofield, J. Electron Spectrosc. 8 (1976) 129–137.
[6] A. Chagnes, B. Carré, P. Willmann, R. Dedryvère, D. Gonbeau, D. Lemordant, J. Electrochem. Soc. 150 (2003) A1255–A1261.
[7] D. Aurbach, Y. Ein-Eli, B. Markovsky, A. Zaban, S. Luski, Y. Carmeli, H. Yamin, J. Electrochem. Soc. 142 (1995) 2882–2889.
[8] Z. Ogumi, A. Sano, M. Inaba, T. Abe, J. Power Source 97/98 (2001) 156–158.
[9] S. Laruelle, S. Pilard, P. Guenot, S. Grugeon, J.-M. Tarascon, J. Electrochem. Soc. 151 (2004) 1202–1209.
[10] R. Dedryvère, S. Laruelle, S. Grugeon, L. Gireaud, J.-M. Tarascon, D. Gonbeau, J. Electrochem. Soc. 152 (2005) A689–A696.
[11] R. Dedryvère, L. Gireaud, S. Grugeon, S. Laruelle, J.-M. Tarascon, D. Gonbeau, J. Phys. Chem. B 109 (2005) 15868–15875.
[12] S. Leroy, F. Blanchard, R. Dedryvère, H. Martinez, B. Carré, D. Lemordant, D. Gonbeau, Surf. Interf. Anal. 37 (2005) 773–781.

[13] A.M. Anderson, D.P. Abraham, R. Haasch, S. Mac Lauren, J. Amine K, J. Electrochem. Soc. 149 (10) (2002) A1358–A1369.
[14] D. Aurbach, B. Markovsky, I. Weisman, E. Levi, Y. Ein-Eli, Electrochim. Acta 45 (1999) 67–86.
[15] P. Novak, F. Joho, M. Lanz, B. Rykart, J.C. Panitz, D. Alliata, R. Kötz, O. Haas, J. Power Sources 97/98 (2001) 39.
[16] M.E. Spahr, H. Buqa, A. Würsig, D. Goers, L. Hardwick, P. Novak, F. Krumeich, J. Dentzer, C. Vix-Guterl, J. Power Sources 153 (2006) 300–311.
[17] (a) E. Wang, D. Ofer, W. Bowden, N. Iltchev, R. Moses, K. Brand, J. Electrochem. Soc. 147 (2000) 4023;
(b) F. Blanchard, Ph.D. Thesis, Université de Tours, France, 2004.